Pergamon

Electrochimica Acta, Vol. 43, Nos 19–20, pp. 2825–2830, 1998

Printed in Great Britain
PII: S0013-4686(98)00023-1
0013-4686/98 $19.00 + 0.00

Cyclic voltammetry and ^{195}Pt nuclear magnetic resonance characterization of graphite-supported commercial fuel cell grade platinum electrocatalysts

Cynthia Rice, Yuye Tong, Eric Oldfield and Andrzej Wieckowski*

Department of Chemistry, University of Illinois at Urbana-Champaign, 600 South Mathews Avenue, Urbana, IL 61801, U.S.A.

(Received in Newcastle 21 January 1998)

Abstract—Three graphite-supported commercial fuel cell grade platinum electrocatalysts with different average particle sizes have been studied by cyclic voltammetry and ^{195}Pt nuclear magnetic resonance (NMR) spectroscopy. There is a strong correlation of platinum particle size with both NMR and cyclic voltammetric lineshapes. From cyclic voltammetric profiles it is possible to observe the transformation to a single crystallite geometry as the particle size increases from 2.0 to 8.8 nm. The particle-size-dependent NMR spectra give the first conclusive assignment of the signals from platinum atoms at surfaces wetted by electrolyte, and provide an opportunity for comparison with spectra from equivalent catalysts in the gas phase. We have also found that the application of multiple voltammetric cycles to such platinum particles increases the particle size. © 1998 Published by Elsevier Science Ltd. All rights reserved

Key words: ^{195}Pt NMR, platinum fuel cell material, cyclic voltammetry.

INTRODUCTION

Extensive investigations utilizing solid state nuclear magnetic resonance (NMR) spectroscopy to probe platinum's reactivity have been performed during the last fifteen years on gas phase platinum catalysts by looking at platinum itself [1–10], as well as at various surface adsorbates such as carbon monoxide and small organic molecules [11, 12]. The NMR work by both Slichter's and van der Klink's groups on ^{195}Pt-NMR using samples of various dispersions has demonstrated characteristic size-dependent NMR spectra [2, 13], from which surface atoms have been assigned. These studies have been on either simple oxide (such as Al_2O_3, TiO_2 or SiO_2) supported or zeolite encapsulated platinum catalysts. However, there has also recently been increasing interest in the use of solid state NMR spectroscopic methods to investigate fuel cell related electrocatalytic systems [13–19], this time in an electrochemical environment. These studies have focused primarily on adsorbed carbon monoxide, a potent platinum electrocatalyst poison. Very recently [19], however, we have also demonstrated the feasibility of using ^{195}Pt-NMR to study graphite-supported commercial fuel cell grade electrocatalysts themselves. This opens the way to gaining a much better understanding of electronic structure and bonding characteristics of platinum electrodes, including such details as CO poisoning, and the reasons for catalytic improvements made by "alloying" platinum with ruthenium.

NMR spectra are strongly effected by the *local* electronic properties, such as Larmor diamagnetism, van Vleck and Curie paramagnetism of localized (orbital) electrons, and Pauli paramagnetism of conduction electrons, which influence the observed nucleus [20, 21]. In metals, the Pauli paramagnetism, determined by the electronic density of states at the Fermi level, is usually the dominant mechanism. The lack of translational symmetry, such as occurs in small metal particles used as catalysts, makes the local density of states at the Fermi level (E_f-LDOS) position dependent, and therefore increases the

*Author to whom correspondence should be addressed.

breadth of the NMR spectrum. For platinum catalysts with clean surfaces in the gas phase, it has been observed that the surface atoms resonate at around 1.100 G/kHz, a value coinciding with the conventional reference for the Knight shift, while the bulk atoms are at 1.138 G/kHz. Such a distinctive surface-like signal is essential for the success of ^{195}Pt-NMR of platinum catalysts in the gas phase. In electrolyte systems, the surface atoms of the electrocatalysts experience a major environmental change, as do their electronic properties, due the presence of the electrical double layer. It is therefore essential to record any specific effects due to the presence of the solution part of the solid/liquid interface. We have recently concluded, based on the great similarity of the ^{195}Pt-NMR spectrum of an electrocatalyst in an electrolyte solution to that in the "gas phase", that the surface-like signals are still around 1.100 G/kHz in an electrochemical environment, as in the gas phase environment. In this paper, we present further evidence which supports such an assignment.

EXPERIMENTAL

All samples were of commercial fuel cell grade platinum supported on vulcanized (XC-72) conductive graphite, and were obtained from E-TEK (Natick, MA). Specific platinum weight percents and the corresponding X-ray diffraction data for the average particle size were obtained from E-TEK.

The platinum catalyst as received was found to be covered by a layer of chemisorbed surface oxide [19]. To remove this oxide layer, approximately 500 mg of the particles were made as a working electrode in an electrochemical cell using a platinum boat. The three-electrode cell, in addition to the Pt-powder working electrode, contained a platinum gauze counter electrode and a 1 M NaCl Ag/AgCl reference electrode. The cell potential was controlled by a PGP201 Potentiostat/Galvanostat manufactured by Radiometer (Villeurbanne, France). The electrolyte used was 0.5 M H_2SO_4 and was prepared from concentrated analytical grade sulfuric acid from Mallinckrodt Baker (Paris, Kentucky) diluted in Milli-pore (Millipore, Bedford, MA) water.

For the oxide reduction process, the potential was held in the double layer region for several hours under a continuous stream of ultra-pure argon. The experiment was completed when the current decreased to a negligible level (μA). Once the oxide film was removed, the particles were transferred, together with a small portion of the electrolyte, into an NMR tube (10 mm diameter × 25 mm length) which was then flame-sealed after several pump/purge cycles with ultra pure nitrogen. After sealing, the sample was frozen in liquid nitrogen, and it remained at this temperature until NMR spectra were recorded.

NMR measurements were carried out using a "home-built" spectrometer, equipped with an 8.47447 T superconducting solenoid magnet (Oxford Instruments, Osney Mead, U.K.), using an Oxford Instruments CF-1200 cryostat. A Hahn spin-echo pulse sequence ($\pi/2$–τ_0–π–τ_0–acquire) with 16-step phase cycling to eliminate ringdown, was used for data acquisition. The value for t_0 was set at 30 μs. The 90° pulse length varied between 4 and 7 ms, depending on the sample loading, and the repetition rate was 50 s^{-1}. The higher Pt-loading sample (8.8 nm) had an enhanced signal/noise ratio (> 10.1 with only 6 000 scans, at the 1.137 G/kHz spectral position) due to the increased platinum abundance. The 2.0 nm particle sample contained less platinum and as expected required many more scans to increase the signal/noise ratio to above 10:1, at 1.100 G/kHz, typically 120 000 scans. Due to the large frequency distribution in the platinum particles, point-by-point spectral determinations were necessary, in which the spectrometer frequency was manually swept between 74.3 and 78 MHz at (typical) intervals of 100 kHz.

RESULTS AND DISCUSSION

Cyclic voltammetry characterization

Cyclic voltammetry with Pt particles was performed in an electrochemical cell (Figure 3) at 20 mV/min using from 50 to 380 mg of platinum particles. The particles sedimented on the top of one another in the Pt boat allowing contact between each Pt particle and the solvent. We found that the cyclic voltammetry current was proportional to the quantity of sample added onto the Pt boat. The proportionality suggests that this experimental arrangement allows each particle to contribute equally to the overall current. The ^{195}Pt-NMR spectra (see below) confirm that the oxide was successfully removed from the catalyst.

Low temperature NMR measurements

In order to increase the weak ^{195}Pt-NMR signal all measurements were carried out at a near liquid nitrogen temperature (80 K), in which the electrolyte solution was frozen. A frozen medium is a legitimate electrolyte in electrochemistry as shown, for instance, by Stimming and Schmickler, since the dynamic charge-carrier transfer across the interfaces is not completely quenched [22]. Likewise, as demonstrated more recently [16] surface diffusion of CO on platinum in frozen media has a very similar activation energy to CO on "dry" (or gas phase) platinum in a similar temperature range. Evidently, surface water ice is seen as a "fluid" for surface molecular motions on the time-scales required for CO surface diffusion. These results therefore

demonstrate that double layer is not significantly modified at low temperatures, and that no significant changes in the electronic structure and properties of platinum electrocatalyst particles are to be expected.

We use for reference ^{195}Pt-NMR spectra obtained on dry, oxide-free Pt samples of various particle size [23]. Figure 1 shows the evolution of such NMR spectra at 80 K as the particle size decreases and the dispersion (the ratio of the number of surface atoms to the total number of platinum atoms) increases [23]. For bulk platinum, there is a single peak at 1.138 G/kHz [7]. With increasing dispersion, the bulk peak broadens out and a new peak centered around 1.100 G/kHz begins to emerge. When the particles are only 1.0 nm in diameter, i.e. with a dispersion of 80–100%, the bulk peak (at 1.138 G/kHz) is no longer observed, and most of the NMR signal intensities is centered around 1.100 G/kHz, giving strong evidence for a surface signal [23]. In contrast, Fig. 2 shows ^{195}Pt-NMR spectra of clean platinum in the frozen media of average particle size 2.0, 2.5 and 8.8 nm. By assuming that the electrocatalyst has an ideal cubooctahedral morphology, the dispersion corresponding to these particle sizes can be computed to be 54%, 45%, and 15% [7]. The variations in the lineshape exhibit a similar trend to that seen in the gas phase (Fig. 1). That is, as the dispersion increases, the peak centered at 1.100 G/kHz increases. This confirms that the signal observed at around 1.100 G/kHz arises from surface atoms of the electrocatalyst, as concluded previously [19]. Note also that characteristic features of platinum oxide [19] are absent.

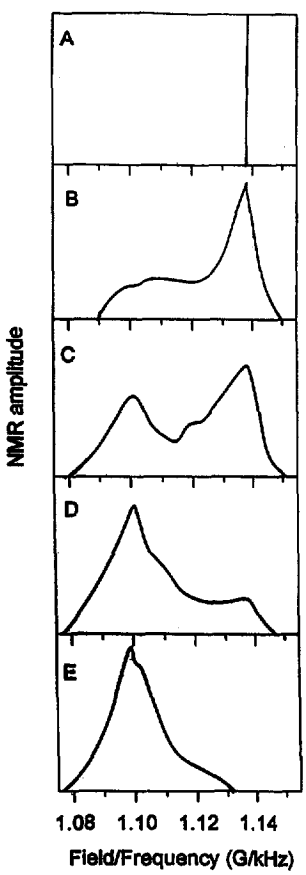

Fig. 1. ^{195}Pt-NMR spectra of various "gas phase" platinum particles having clean surfaces. (A) Pt bulk, 10 μm; (B) Pt/SiO_2, colloidal process, 48 Å, 22%; (C) Pt/TiO_2, colloidal process, 27 Å, 36%; (D) Pt/TiO_2, ion exchange, 17 Å, 60%; (E) Pt/Al_2O_3, impregnation, 10 Å, 80–100%. Adapted from Ref. [23]

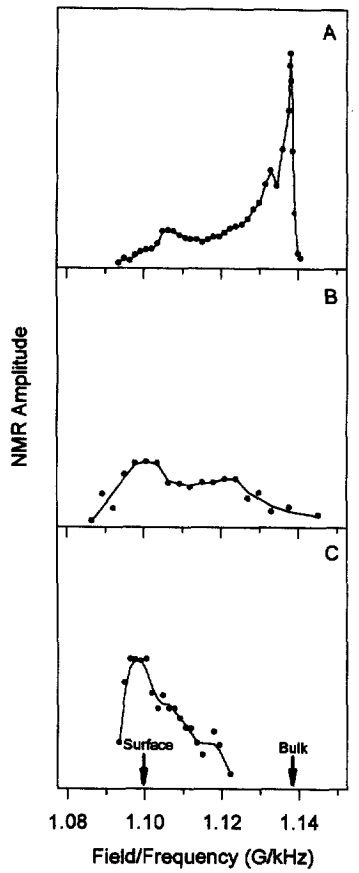

Fig. 2. 8.47 T ^{195}Pt-NMR spectra of commercial graphite-supported platinum electrodes cleaned in 0.5 M H_2SO_4 with potential held at 250 mV. (A) 8.8 nm particle; (B) 2.5 nm particles and (C) 2.0 nm diameter particles. Spectra were recorded point-by-point at 80 K. All spectra were normalized to the same area.

Spectral interpretation

By comparing the spectra shown in Figs 1 and 2, in dry and frozen environments, respectively, it can be seen that there is a major difference between the two sets of samples, even though the surfaces in both samples are clean and oxide-free. Specifically, there is a clear low-field shift of the bulk-like signal as the particles become smaller. In the dry case, even for dispersions as high as 60%, the bulk-like

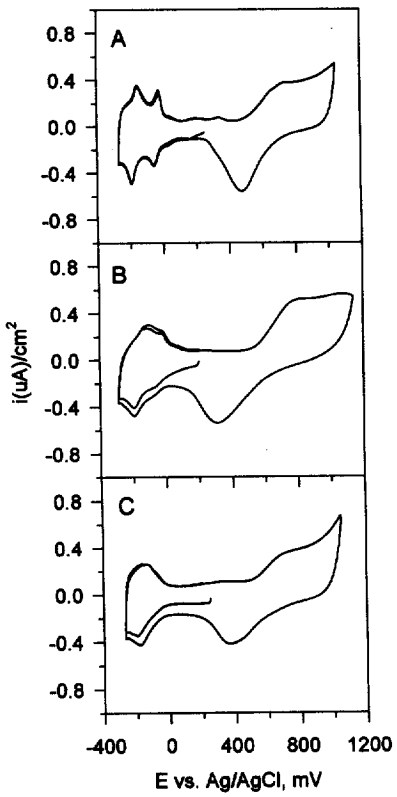

Fig. 3. Cyclic voltammograms of commercial graphite-supported platinum electrodes in 0.5 M H_2SO_4 at a sweep rate of 20 mV/min vs an Ag/AgCl reference electrode, for the following platinum particle diameters: (A) 8.8 nm; (B) 2.5 nm; and (C) 2.0 nm.

signals are hardly shifted (Fig. 1(D)), while in the electrolyte medium, even at a dispersion of 45%, only a small signal can be seen at 1.138 G/kHz, since the high-field (bulk) peak is now shifted to 1.123 G/kHz.

An ideal 8.8 nm platinum cubooctahedral particle has ~20 layers and ~29 000 atoms. In contrast, a 2.5 nm particle has 6 layers and ~500 atoms, and a 2.0 nm particle has 5 layers and ~300 atoms. In Ref. [19], using 2.5 nm particles, we found that there was a major enhancement of the s-like E_f-LDOS at the electrocatalyst surface in electrolyte solutions. The 8.8 nm sample shown in Fig. 2(A) has a bulk-like peak at exactly 1.138 G/kHz. Since the resonance position for a given Pt atom in a particle is determined by the sum of the positive s-like and negative d-like hyperfine fields at the nucleus [24], it is reasonable to correlate the low-field shift of the "bulk-like" signals observed with the smaller particles to an s-like E_f-LDOS enhancement at the surface, which then shifts the sub-surface and sub-sub-surface layer signals to lower field positions. The fact that the effect is quite long-range (~5 layers, see Fig. 3(C)) emphasizes the delocalized character of the enhanced E_f-LDOS, consistent with the s-like character of the conduction electrons.

Voltammetric interpretation

Since the seminal work of Conway and co-workers [25], cyclic voltammetry has been widely used to characterize platinum surfaces in a variety of electrochemical environments. Cyclic voltammograms obtained in this paper (Fig. 3) were normalized to the surface area within each sample, from the mass of platinum used and the dispersion value obtained from the model calculation (see Table 1). Qualitatively, the cyclic voltammetric (CV) curves studied here show similarities to those obtained with 15 nm platinum particles supported on the basal plane of graphite [26]. However, the CV profiles are clearly sensitive to particle dispersion (Fig. 3). The major effect is an increase in the irreversibility of surface oxide reduction, or the decrease in the oxide reduction rate. This occurs to such an extent that the reduction process at 20 mV/min is not complete until the hydrogen evolution edge is reached (cf. the negative going scans, first and second in Fig. 3(B),(C)). The oxygen evolution reaction seems to begin at a lower potential on the smallest particles (Fig. 3(C)), but more work is needed to confirm this effect. The CV profiles characteristic of hydrogen adsorption/desorption are also particle size dependent, and show a correlation between microscopic roughness and charge generation, due to proton/hydrogen, reduction/oxidation processes, respectively. Small particles (2.0 nm) have rougher surfaces than do larger particles, due to the prevalence of corners and edges. This induces random Pt–hydrogen bond formation, causing a variety of overlapping CV features, including the tailing oxide reduction process (Fig. 3(C)). Collectively, these microscopic and chemical features completely suppress strongly-bonded hydrogen formation [25]. In contrast, larger particles (8.8 nm) more closely resemble disordered single crystals surfaces and yield two well resolved peaks. Those correspond to weakly- and strongly-bonded hydrogen, in both the forward and reverse cycles (Fig. 3(A)). The sample with the medium particle size (2.5 nm) shows, as expected, an intermediate behavior (Fig. 3(B)).

Table 1.
Dispersion values for E-TEK Pt electrocatalysts as determined from model building, cyclic voltammetry, and ^{195}Pt-NMR.

Average diameter (Å)	Cubooctahedral model (%)	CV (%)	NMR (%)
88	15	15	17
25	45	43	50
20	54	68	66

Catalyst dispersion

Evaluating platinum dispersion is clearly important for the correct interpretation of both NMR and CV experiments and can be achieved in three ways: from the hydrogen adsorption charge; from physical measurements, such as transmission electron microscopy or X-ray diffraction and from ^{195}Pt-NMR [2, 7]. In this paper, the dispersion from cyclic voltammetry is obtained as follows: The charge per unit area is determined from the area under the hydrogen desorption portion of the CV curve (1.6×10^{-16} μC/H site), from which the number of surface hydrogen sites is determined. The total number of platinum atoms in the sample is then obtained, since the mass and percent platinum are known (the contribution to the current from the Pt boat was always less than 0.5% and can therefore be neglected). If the stoichiometry of H/Pt = 1 for hydrogen adsorption is used, the dispersion can then be calculated. To estimate the dispersion from the NMR spectra, we calculate the ratio of the spectral area lower than 1.110 G/kHz to the total spectral area. Since our spectra have not been corrected for the T_2 effects [6], this procedure may *overestimate* the dispersion somewhat, but the effect appears to be very small, as we show below.

For a physical measurement method, we took the average particle sizes and calculated the ratio of the number of surface atoms to the number of total atoms, assuming an ideal cubooctahedral form. Table 1 collects the results of all three types of calculation, which are clearly in very good accord with each other. Since XPS data on small platinum particles, ranging from 2.0 to 8.0 nm, have shown that the surfaces are virtually free of surface contamination [27], the higher dispersion obtained from the hydrogen portion of the CV curve for the 10% Pt sample may relate to the fact that the actual stoichiometry of H/Pt is higher that 1 for small particles on heterogeneous catalysts (28). These results are, important since they strongly support the ^{195}Pt-NMR peak assignments, based on both simple model building arguments, and the results from cyclic voltammetry.

The effect of repetitive CV scans

Finally, we show in Fig. 4 the ^{195}Pt-NMR spectra of two clean surface samples but prepared in different ways from the *same* "as-received" sample (20% Pt loading on graphite). Sample B was cleaned by extensive potential cycling [19], while sample A (the same as in Fig. 2(B)) was cleaned by holding the potential at 250 mV (within the double layer region) until the reduction current could no longer be measured. The dispersion estimated from the sample shown in spectrum B is 27%, indicating relatively large particles, while spectrum A gave a dispersion of 50%, consistent with the average particle size of the as-received sample as measured by X-ray diffraction*. This dispersion lowering provides strong evidence for sintering produced by potential cycling, an effect which clearly needs to be borne in mind when analyzing the results of both adsorbate (surface ligand) and metal electrochemical NMR experiments.

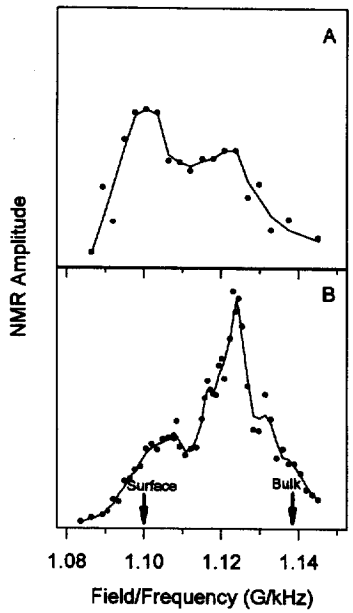

Fig. 4. ^{195}Pt-NMR spectra of commercial graphite-supported platinum electrodes. (A) held at a 250 mV without potential cycling during cleaning; (B) Cleaned by extensive potential cycling.

CONCLUSIONS

By combining cyclic voltammetry and ^{195}Pt-NMR, we have demonstrated a promising new approach to characterizing commercial graphite-supported platinum fuel cell electrocatalysts, in an electrochemical environment. The ^{195}Pt-NMR spectra of a small platinum particle electrocatalyst on conductive (graphite) supports in the liquid phase show similar lineshapes and particle size dependencies to those found in the gas phase. However, while the surface-like signals overlap those seen in the gas phase (at around 1.100 G/kHz), the bulk-like signals in *smaller* particles are shifted to the lower field position. This appears to be due to the enhancement of the s-like E_f-LDOS observed at the electrocatalyst surface [19]. Platinum CVs are also particle size dependent. Larger particles (8.8 nm) produce cyclic voltammograms characteristic of disordered single crystal surfaces, while for smaller particles having rougher surfaces (due to dominant corner and edge atoms), the voltammograms show

*Particle size information provided by E-TEK, 6 Mercer Rd., Natick, MA, 01970. Phone: +1-508-653-9331.

no such single crystal features. This particle size dependence of the CV results may be of practical use in monitoring the morphological evolution of fuel cell electrocatalysts. And finally, from the change of the ^{195}Pt-NMR lineshape, we have found clear evidence that the application of multiple voltammetric cycles produces sintering effects in the supported platinum electrocatalysts.

ACKNOWLEDGEMENTS

This work was supported by the Department of Energy, grant DEFG02-96ER45439, administered by the Frederick Seitz Materials Research Laboratory at the University of Illinois and by the National Science Foundation under Grant CHE 97-00963 and by the U.S. Department of Defense, DARPA grant DAAH-95-0581.

REFERENCES

1. I. Yu, A. A. V. Gibson, E. R. Hunt and W. P. Halperin, *Phys. Rev. Lett.* **44,** 384 (1980).
2. H. E. Rhodes, P.-K. Wang, H. T. Stokes, C. P. Slichter and J. H. Sinfelt, *Phys. Rev. B* **26,** 3559 (1982).
3. H. E. Rhodes, P.-K. Wang, C. D. Makowka, S. L. Rudaz, H. T. Stokes, C. P. Slichter and J. H. Sinfelt, *Phys. Rev. B* **26,** 3569 (1982).
4. H. T. Stokes, H. E. Rhodes, P.-K. Wang, C. P. Slichter and J. H. Sinfelt, *Phys. Rev. B* **26,** 3575 (1982).
5. J. J. van der Klink, J. Buttet and M. Graetzel, *Phys. Rev. B* **29,** 6352 (1984).
6. J. P. Bucher and J. J. van der Klink, *Phys. Rev. B* **38,** 11038 (1988).
7. J. P. Bucher, J. Buttet, J. J. van der Klink and M. Graetzel, *Surf. Sci.* **214,** 347 (1989).
8. Y. Y. Tong, D. Laub, G. Schulz-Ekloff, A. J. Renouprez and J. J. van der Klink, *Phys. Rev. B* **52,** 8407 (1995).
9. Y. Y. Tong, A. J. Renouprez, G. A. Martin and J. J. van der Klink, in *Studies in Surface Science and Catalysis*, 101 (part B) (*11th International Congress on Catalysis, 40th Anniversary*), ed. J. W. Hightower, W. N. Delgass, E. Iglesia and A. T. Bell. Elsevier, Amsterdam, 1996, p. 901.
10. Y. Y. Tong, J. Billy, A. J. Renouprez and J. J. van der Klink, *J. Am. Chem. Soc.* **119,** 3929 (1997).
11. P.-K. Wang, J.-P. Ansermet, S. L. Rudaz, Z. Wang, S. Shore, C. P. Slichter and J. H. Sinfelt, *Science* **234,** 35 (1986).
12. C. P. Slichter, *Ann. Rev. Phys. Chem.* **37,** 25 (1986).
13. J. P. Bucher, J. Buttet, J. J. van der Klink, M. Graetzel, E. Newson and T. B. Troung, *Colloids and Interfaces* **36,** 155 (1989).
14. W. H. Chan and A. J. Wieckowski, *Electrochem. Soc.* **137,** 367 (1990).
15. P. J. Slezak and A. J. Wieckowski, *Magn. Reson. A* **102,** 166 (1993).
16. J. B. Day, P. A. Vuissoz, E. Oldfield, A. Wieckowski and J.-Ph. Ansermet, *J. Am. Chem. Soc.* **118,** 13046 (1996).
17. J. J. Wu, J. B. Day, K. Franaszczuk, B. Montez, E. Oldfield, A. Wieckowski, P.-A. Vuissoz and J. P. Ansermet, *J. Chem. Soc. Faraday Trans.* **93,** 1017 (1997).
18. M. S. Yahnke, B. M. Rush, J. A. Reimer and J. Cairns, *J. Am. Chem. Soc.* **118,** 12250 (1996).
19. Y. Y. Tong, C. Belrose, A. Wieckowski and E. Oldfield, *J. Am. Chem. Soc.* **119,** 11709 (1997).
20. A. Abragam, *Principles of Nuclear Magnetism*. Oxford University Press, 1961.
21. C. P. Slichter, *Principles of Magnetic Resonance*, 3rd edition. Springer, Berlin, 1990.
22. U. Stimming and W. Schmickler, *J. Electroanal. Chem.* **150,** 125 (1983).
23. J. P. Bucher, Ph.D. thesis, École Polytechnique Fédérale de Lausanne, Lausanne, Switzerland, 1988.
24. Y. Yafet and V. Jaccarino, *Phys. Rev.* **133A,** 1630 (1964).
25. H. Angerstein-Kozlowska, B. E. Conway and W. B. A. Sharp, *J. Electroanal. Chem.* **43,** 9 (1973).
26. P. A. Christensen, A. Hamnett, J. Munk and G. L. Troughton, *J. Electroanal. Chem.* **370,** 251 (1994).
27. P. J. Slezak, Ph.D. thesis. University of Illinois at Urbana-Champaign, Champaign, IL, 1992.
28. D. M. Cox, P. Fayet, R. Brickman, M. Y. Hahn and A. Kaldor, *Catal. Lett.* **4,** 271 (1990).